Improving Channel Mobility in Graphene-FETs by Minimizing Surface Phonon Scattering - A Simulation Study

Xinxin Yu, Jiahao Kang, Jinyu Zhang*, Lilin Tian, and Zhiping Yu
Institute of Microelectronics, Tsinghua University
Beijing, China 100086
zhangjinyu@tsinghua.edu.cn

***Abstract*—In graphene-based field-effect transistors (graphene FETs), the carrier channel mobility is strongly influenced by substrate and gate dielectric materials. In this paper, we theoretically investigated the carrier channel mobility for the graphene-FET. Surface phonon (SP) scattering, screened Coulomb scattering, acoustic phonon and optical phonon scattering mechanisms are considered in the mobility calculation. Applying Mahan's theory, the SP scattering in a gate stack structure is evaluated. It is found that SP scattering plays an important role especially in high-k dielectrics. The charged impurity and SP scattering can be suppressed effectively by inserting a polymer layer between the gate dielectric and graphene. The thickness of the ploymer layer, however, should be carefully selected to balance the channel carrier mobility enhancement and gate control ability. Our calculation results are consistent with previous calculations and experimental observations.**

Keywords—graphene-FET; polymer; surface phonon scattering; mobility

I. INTRODUCTION

Graphene could be a promising material to fabricate high performance transistors due to its ultra high mobility. However, surface phonons and charged impurities scattering greatly reduce the carrier channel mobility in graphene-based field-effect transistors (FETs) [1]. Even though high-k dielectric used as the gate insulator can screen the impurities Coulomb scattering, surface phonon (SP) scattering caused by the high-k material at the dielectric/graphene interface may impair the mobility enhancement achieved by charged impurity screening. Recently IBM succeeds to achieve high field-effect carrier mobility in graphene transistors by adding a low-k polymer buffer layer between high-k dielectric and graphene to minimize charged impurity and SP scattering[2].

Unlike acoustic and optical phonons in bulk graphene [3] or graphene ripples [4], SPs are an extrinsic source of scattering that depends on the thermal excitation of contact surfaces [5]. Several recent works have pointed out that the remote phonons in high-k dielectrics are more easily to coupling with the plasmon in the channel due to the polar nature and soft energy bonds. This feature presents itself not only in graphene, but in carbon nanotubes [6], as well as in the metal-oxide-semiconductor field effect transistors (MOSFETs) [7]. However, the SP scattering is of lesser importance in the conventional MOSFETs, as in graphene due to the much smaller vertical dimension of the devices given by the graphene layer. In this work, the mobility in top gated graphene-FET channel is studied associated with adding a low-k NFC polymer buffer layer [2]. Different scattering mechanisms are considered including screened Coulomb scattering, intrinsic acoustic phonon and optical phonon scattering, and SP scattering. Carrier mobility and electrical resistivity are obtained as a function of gate voltage.

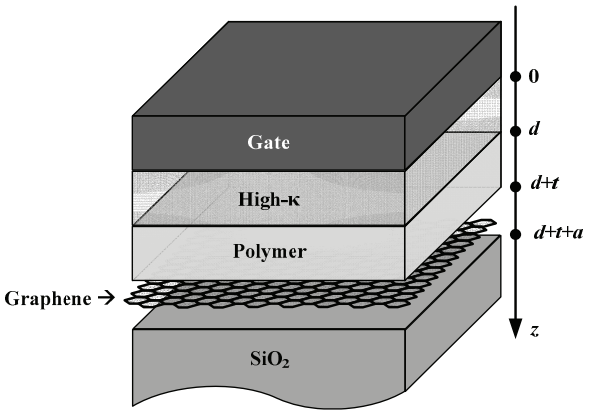

Fig. 1. Schematic representation of the graphene-FET with a polymer buffer layer. In this work, the thicknesses of high-κ and polymer insulator are both 10 nm [1]. The thickness of graphene layer is 0.68 nm. The gate is considered to be an ideal metal.

II. SCATTERING MECHANISMS MODEL

A. Graphene-FET structure

Fig. 1 shows the structure considered in this work. SiO_2 is taken as a semi-infinite substrate and a single layer of graphene is placed on top of the oxide. A buffered polymer layer and a HfO_2 layer are subsequently deposited on the top of the graphene sheet.

B. Surface Phonon modes

There are three types of modes in this structure: transverse-optical (TO) modes, longitudinal-optical (LO) modes and surface-optical (SO) modes. Since electric field produced by the TO and LO phonons is zero outside the dielectric, the electron in graphene interacts only with surface modes. Due to the polymer is a low-k material

(ε=2.4), the SO scattering of the polymer layer is ignored in this work. It is assumed that both SiO_2 and high-k dielectrics are semi-infinite neglecting influence of the metal gate on the carrier mobility in the graphene channel because of large gate dielectric thickness. Two phonon modes exhibiting the largest oscillator strength are considered in the gate and substrate dielectric [6]. The frequency dependence of the dielectric constant can be written as

$$\varepsilon_{ox}(\omega)=\varepsilon_{ox}^{\infty}+\frac{\varepsilon_{ox}^{i}-\varepsilon_{ox}^{\infty}}{1-\omega^2/\omega_{TO2}^2}+\frac{\varepsilon_{ox}^{0}-\varepsilon_{ox}^{i}}{1-\omega^2/\omega_{TO1}^2} \tag{1}$$

where the subscript ox is for general dielectric. ε_{ox}^{0} and $\varepsilon_{ox}^{\infty}$ are static and optical permittivity of the dielectric, respectively. ω_{TO1} and ω_{TO2} are the angular frequencies of two transverse optical phonon modes. ε_{ox}^{i} is an intermediate permittivity describing the dielectric response at some intermediate frequency ω_{int}. Table I provides dielectric constants at different frequencies for SiO_2 and HfO_2.

TABLE I. DIELECTRIC CONSTANT FOR SEVERAL MATERIALS[6].

Quantity	Dielectric	
	SiO_2	HfO_2
ε_{ox}^{0}	3.90	22.00
ε_{ox}^{i}	3.05	6.58
$\varepsilon_{ox}^{\infty}$	2.50	5.03

The dielectric response of graphene is neglected since charges in graphene merely screen the electric field lines originating from the oxide-graphene interface [8]. Applying the boundary conditions at each interface, the secular equation can be written as

$$\begin{aligned}&(\varepsilon_{Si}-\varepsilon_p)e^{-2qt}\left[(\varepsilon_p+\varepsilon_h)e^{-2qd}-(\varepsilon_p-\varepsilon_h)\right]\\&=(\varepsilon_{Si}+\varepsilon_p)\left[(\varepsilon_p+\varepsilon_h)-(\varepsilon_p-\varepsilon_h)e^{-2qd}\right]\end{aligned} \tag{2}$$

where ε_{Si}, $\varepsilon_p$and ε_h refer to the dielectric response of SiO_2, polymer, and HfO_2. ε_{Si} and ε_h are functions of frequency as shown in Eq. 1, and ε_p equals to 2.4. The thickness of the gate dielectric and polymer layer is denoted by d and t, respectively. The SP modes dispersion in the presence of the polymer layer is solved from Eq. 2. Without the polymer layer, the secular equation can be simplified as

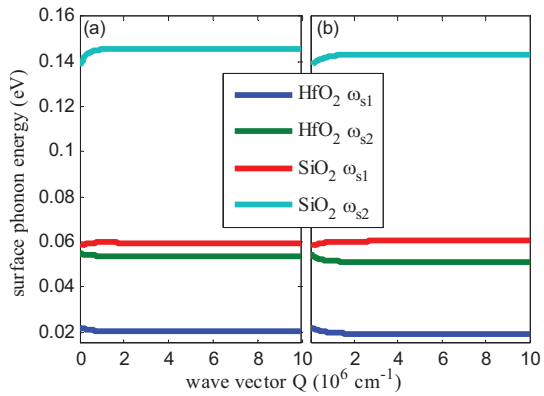

Fig. 2. Phonon energy dispersion of (a) SiO_2/polymer /HfO_2/Metal structure and (b) SiO_2/HfO_2 /Metal structure.

$$(\varepsilon_{Si}-\varepsilon_h)e^{-2qd}=\varepsilon_{Si}+\varepsilon_h \tag{3}$$

which is identical to Eq. 2 when t=0. The phonon dispersion with and without the polymer layer is shown in Fig. 2. It can be seen that the SP modes are nearly dispersionless and the polymer has little effects on SP energies. Note that the SO coupling between SiO_2 and HfO_2 is not considered in this work. The carrier mobility in graphene caused by the SP scattering from SiO_2 and HfO_2 is calculated separately.

C. SP scattering

Following Mahan's theory [9], we calculate the dielectric SP scattering rate. The polarization field for mode $\boldsymbol{q}$ in position $\boldsymbol{R}=(x\hat{x}+y\hat{y}+z\hat{z})$ of the dielectric can be expressed as

$$\boldsymbol{P}_{\boldsymbol{q}}(\boldsymbol{R})=\sum_{i=1}^{2}F_i\times\left[\boldsymbol{g}_{\boldsymbol{q}}(\boldsymbol{R})a_{-\boldsymbol{q}}^{\dagger}+\text{H.c.}\right] \tag{4}$$

where $a_{-\boldsymbol{q}}^{\dagger}$ is the creation operator for mode $\boldsymbol{q}$ and H.c. is the hermitian conjugate. The amplitude of the dielectric polarization at point $\boldsymbol{R}$ for mode $\boldsymbol{q}$ has the form:

$$\boldsymbol{g}_{\boldsymbol{q}}(\boldsymbol{R})=|\boldsymbol{q}|^{1/2}\left(\frac{\boldsymbol{q}}{|\boldsymbol{q}|}-i\hat{z}\right)e^{|\boldsymbol{q}|z+i\boldsymbol{q}\cdot\boldsymbol{R}} \tag{5}$$

The proportional constant F_i (i=1,2) is calculated for each mode as

$$F_i=\left[\left(\frac{1}{\varepsilon^{\infty}+\varepsilon_s^{\infty}}-\frac{1}{\varepsilon^{0}+\varepsilon_s^{\infty}}\right)\frac{\hbar\omega_{si}}{2\pi A}\right]^{1/2} \tag{6}$$

where A is the normalization factor. ω_{s1} and ω_{s2} are the surface phonon frequency obtained from Table I. ε^{∞} and ε^{0} are the dielectric constant at high and low frequencies for each mode, respectively. ε_s^{∞} is the high frequency dielectric constant of the graphene background lattice replacing '1' (the vacuum dielectric constant) in Mahan's work. By applying the theories of image charges [10] and ignoring the thickness of graphene, ε_s^{∞} is the mean value of high frequency dielectric constants of two dielectrics adjacent to the graphene layer.

The potential caused by SO phonon modes on graphene is calculated by

$$V_i(x,y,a)=\int_{\Omega}d\boldsymbol{R}\frac{(\boldsymbol{r}-\boldsymbol{R})\cdot\boldsymbol{P}_{\boldsymbol{q}}(\boldsymbol{R})}{|\boldsymbol{r}-\boldsymbol{R}|^3} \tag{7}$$

Using the Fourier transform, interaction matrix elements can be acquired as

$$\begin{aligned}V_{i,\boldsymbol{k}\boldsymbol{k}',\boldsymbol{q}}&=\langle\varphi_{\mathbf{k}}|V_i|\varphi_{\mathbf{k}'}\rangle\\&=2\pi eF_iq^{-1/2}e^{-qt}\delta_{\mathbf{k}',\mathbf{k}+\mathbf{q}}\cos\left(\frac{\theta}{2}\right)\end{aligned} \tag{8}$$

where $\mathbf{k}$ and $\mathbf{k}'$ are wave number of the initial state and final state, respectively. θ is the scattering angle. $\varphi_{\boldsymbol{k}}$ and

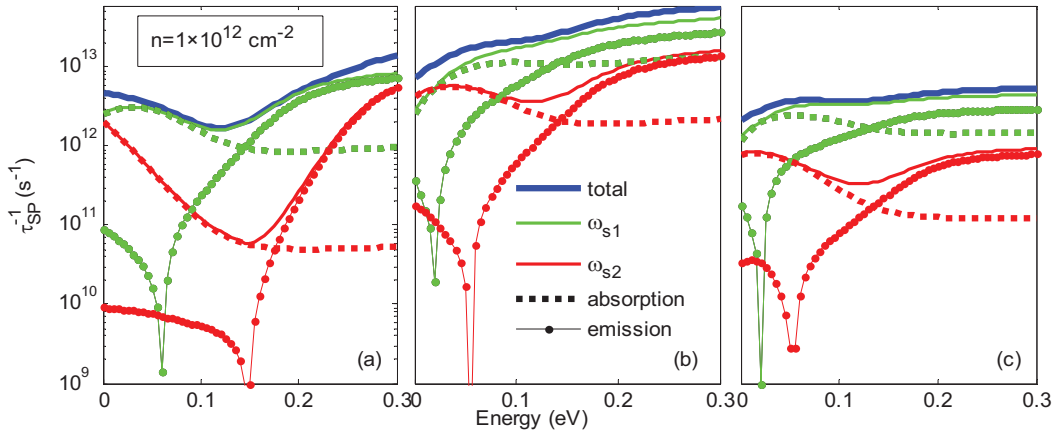

Fig. 3. Channel carrier relaxation time of (a) SiO_2 SP scattering aroused from the SiO_2 substrate, HfO_2 SP scattering in (b) SiO_2/HfO_2/Metal and (c) SiO_2/polymer/HfO_2/Metal structures. The SP scattering includes phonon absorption and emission of each mode. The carrier density set to 1×10^{12} cm^{-2}.

$\varphi_{\boldsymbol{k}'}$ are the electron wave functions of graphene close to the Dirac points:

$$\varphi_{\mathbf{k}} = \frac{e^{i\mathbf{k}\cdot\mathbf{r}}}{\sqrt{2A}}\begin{pmatrix} e^{-i\phi} \\ 1 \end{pmatrix} \tag{9}$$

where ϕ is the angle of $\mathbf{k}$ direction relative to x-axis. The scattering relaxation time is obtained by

$$\frac{1}{\tau(\mathbf{k})} = \frac{\hbar}{2\pi}\sum_{\mathbf{q},i}\left|\frac{V_{i,\mathbf{k}\mathbf{k}',\mathbf{q}}}{\varepsilon_t}\right|^2 \times\Big[n_{\mathbf{q},i}\delta\left(E_{\mathbf{k}} - E_{\mathbf{k}'} - \hbar\omega_{si}\right) + \left(n_{\mathbf{q},i}+1\right)\delta\left(E_{\mathbf{k}} - E_{\mathbf{k}'} + \hbar\omega_{si}\right)\Big] \tag{10}$$

where $n_{\boldsymbol{q},i} = 1/(\exp(\hbar\omega_{si}/kT) - 1)$ is phonon number. ε_t is Thomas-Fermi screening factor of 2D carriers taken from Ref. [11].

The mobility is calculated from $\mu = \sigma/en$ where n is the electron density obtained by solving 1D Possion equation of this structure along z direction. The conductivity is calculated by

$$\sigma = \frac{4e^2}{h}\int_0^{\infty}\tau(E)v_F(E)\left(-\frac{\partial f(E)}{\partial E}\right)dE \tag{11}$$

where v_F is the Fermi velocity and $f(E)$ is the Fermi-Dirac distribution. For graphene, $E_{\mathbf{k}}=\hbar v_F|\mathbf{k}|$.

D. Other scattering Mechanisms

In addition to SP scattering mechanism, screened Coulomb scattering, acoustic phonon (AP) and optical phonon (OP) scattering are considered in the total mobility calculation. The screened Coulomb scattering from SiO_2 is calculated based on Ref.[12]. The matrix element of the scattering potential is given by

$$V_{Coul,\mathbf{k}\mathbf{k}'} = \frac{2\pi e^2 e^{-qd}/(\kappa q)\cos(\theta/2)}{1+v_c(\mathbf{q})\left[1-G(\mathbf{q})\right]\Pi(\mathbf{q})} \tag{12}$$

where κ is an effective background lattice dielectric constant. d is the location of impurities. $\Pi(\mathbf{q})$ is the polarizability function of graphene got from Ref. [1]. $v_c(\mathbf{q})$ is the Coulomb interaction and $G(\mathbf{q})$ is the local field correction. The scattering rate for the screened Coulomb scattering is then obtained as

$$\frac{1}{\tau_{Coul}(E_{\mathbf{k}})} = \frac{2\pi}{\hbar}\sum_a n_i^{(a)}\int\frac{d^2k'}{(2\pi)^2}\left|V_{Coul,\mathbf{k}\mathbf{k}'}\right|^2 \times\left[1-\cos(\theta)\right]\delta\left(E_{\mathbf{k}} - E_{\mathbf{k}'}\right) \tag{13}$$

The mobility calculation is the same as SP scattering described in section *C*.

The mobility for AP and OP scattering can expressed as [13]

$$\mu_{ac} = \frac{e\rho_m\hbar v_F^2 v_{ph}^2}{2\pi D_{ac}^2}\frac{1}{nk_BT}$$
$$\mu_{op} = \frac{e\rho_m v_F^2\omega_{op}}{2\pi D_{op}^2}\frac{1}{nN_{op}} \tag{14}$$

where ρ_m is graphene mass density, n is the carrier concentration, v_{ph} is a characteristic sound velocity, D is the deformation potential for APs and Ops, ω_{op} refers to the OP frequency and N_{op} is the Bose-Einstein occupation number of optical phonons.

The total mobility is given by

$$\frac{1}{\mu_{all}} = \frac{1}{\mu_{SP}} + \frac{1}{\mu_{AP}} + \frac{1}{\mu_{OP}} + \frac{1}{\mu_{Coul}} \tag{15}$$

III. Results and Discussions

As shown in Fig. 2, there are four modes of SPs. High-k dielectric introduces two lowest energy phonon modes which play a dominant role on the channel mobility degradation.

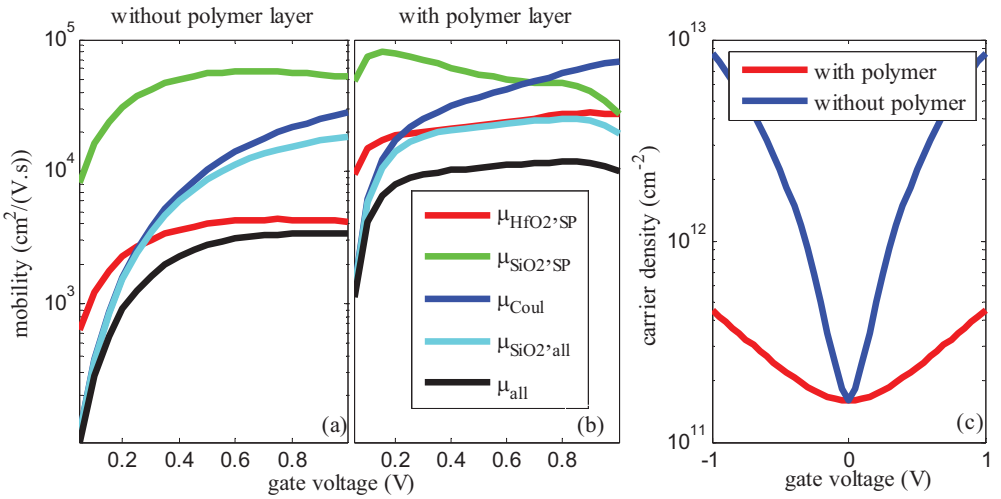

Fig. 4. Relationships of different mobility components and applied gate voltage for (a) SiO_2/HfO_2/Metal Gate and (b) SiO_2/polymer/HfO_2/Metal Gate structures. The total mobility is calculated using Matthiessen's rule including all the scattering mechanisms. $\mu_{SiO2,\,all}$ is the total mobility only aroused from the SiO_2 substrate, which is calculated by just adding SP scattering and screened Coulomb scattering of SiO_2. (3) is the relationship of the carrier density and gate voltage.

Fig. 3 (a) shows the influence of SP scattering for SiO_2. The reciprocal of relaxation time of emission phonon scattering has the minimum when the energies approach to SO phonons energies. Compared with Fig. 3(b), the SP scattering of SiO_2 is much smaller than that of HfO_2 due to higher SO phonon energies. By adding a polymer layer, the reciprocal of the carrier relaxation time decreases significantly, leading to an improved mobility. This mobility enhancement is due to the exponential decay of the SP scattering rate as the increase of the distance between the graphene and gate dielectric surface.

In Figs. 4 (a) and (b), the mobility dependence on the gate voltage is evaluated in our model. A 1D Poisson equation along z axis is solved to get the carrier concentration under a given gate voltage. The average mobility due to the SiO_2 substrate is 9×10^3 $cm^2/V\cdot s$ consistent with the experimental result of 8500 $cm^2/V\cdot s$ [1]. Without the polymer layer, the mobility is mostly confined by the SP scattering of high-k materials and the average mobility is reduced to 2×10^3 $cm^2/V\cdot s$, which is consistent with the previous calculation of 2×10^3 $cm^2/V\cdot s$ [5]. With polymer interfacial layer, the mobility is increased to 8×10^3 $cm^2/V\cdot s$, close to the experiment results of 7.3×10^3 $cm^2/V\cdot s$ [2]. This improvement clearly shows that the polymer attenuates the impact of high-k dielectrics. Note that the polymer layer has a rather low dielectric constant leading to a degradation of the gate control ability. For the experimental structure (10 nm polymer + 10nm HfO_2), the gate capacitance decreases but the total mobility increases by about 4 times in comparison to the structure without the polymer layer. To increase the total conductivity, the thickness of the polymer layer should be carefully selected to balance the total mobility improvement and the gate control ability. The influence of the polymer layer on the device operation performance such as transconductance will be addressed in our future work.

IV. Conclusions

We studied the carrier mobility in a graphene-FET. Various scattering mechanisms are calculated to get the total carrier mobility. Mahan's theory is used to evaluate the SP scattering rate. It is found that SP scattering plays an important role especially in high-κ dielectrics. To suppress the SP scattering, a low-k polymer layer is inserted between the high-κ dielectric layer and graphene. The total mobility increases significantly compared with that without a polymer layer. It is a tradeoff between the increase of the mobility and gate control ability by adding this polymer layer. Our calculation results are consistent with previous calculations and experimental results.

Reference

[1] E. H. Hwang and S. Das Sarma, Phys. ReV. B **77**, 115449 (2008).

[2] D. B. Farmer, H.-Y. Chiu, Y.-M. Lin, K. A. Jenkins, F. Xia, and P. Avouris, Nano Lett. **9**, 4474(2009).

[3] S. V. Morozov, K. S. Novoselov, M. I. Katsnelson, F. Schedin, D. C. Elias, J. A. Jaszczak, and A. K. Geim, Phys. Rev. Lett. 100, 016602(2008).

[4] S. Fratini and F. Guinea, Phys. Rev. B **77**,195415 (2008).

[5] V. Perebeinos, S. V. Rotkin, A. G. Petrov, and P. Avourist, Nano Lett.**9**, 1 (2009).

[6] M. V. Fischetti, D. A. Neumayer, and E. Cartier, J. Appl. Phys. **90**, 4587 (2001).

[7] J. H. Chen, C. Jang, S. Xiao, M. Ishigami, and M. S. Fuhrer, Nat. Nanotechnol. 3, 206(2008).

[8] A. Konar, T. Fang, and D. Jena, arXiv:0902.0819v1(2009).

[9] S. Q. Wang and G. D. Mahan, Phys. Rev. B **6**, 4517 (1972).

[10] G. D. Mahan, Phys. Rev. B **6**,4517 (1972).

[11] E. H. Hwang and S. Das Sarma, Phys. Rev. B 75, 205418 (2007).

[12] S. Adam, E. H. Hwang, E. Rossi, and S. Das Sarma, Solid State Commun. 149, 1072 (2009).

[13] V. Perebeinos and P. Avouris, arXiv:0910.4665v1 (2009).